International Conference on Innovative Applied Energy (IAPE'19) conference, St Cross College, University of Oxford, United Kingdom, 14-15 March 2019.

COMPUTATIONAL FLUID DYNAMIC SIMULATION OF A SOLAR ENCLOSURE WITH RADIATIVE FLUX AND DIFFERENT METALLIC NANO-PARTICLES

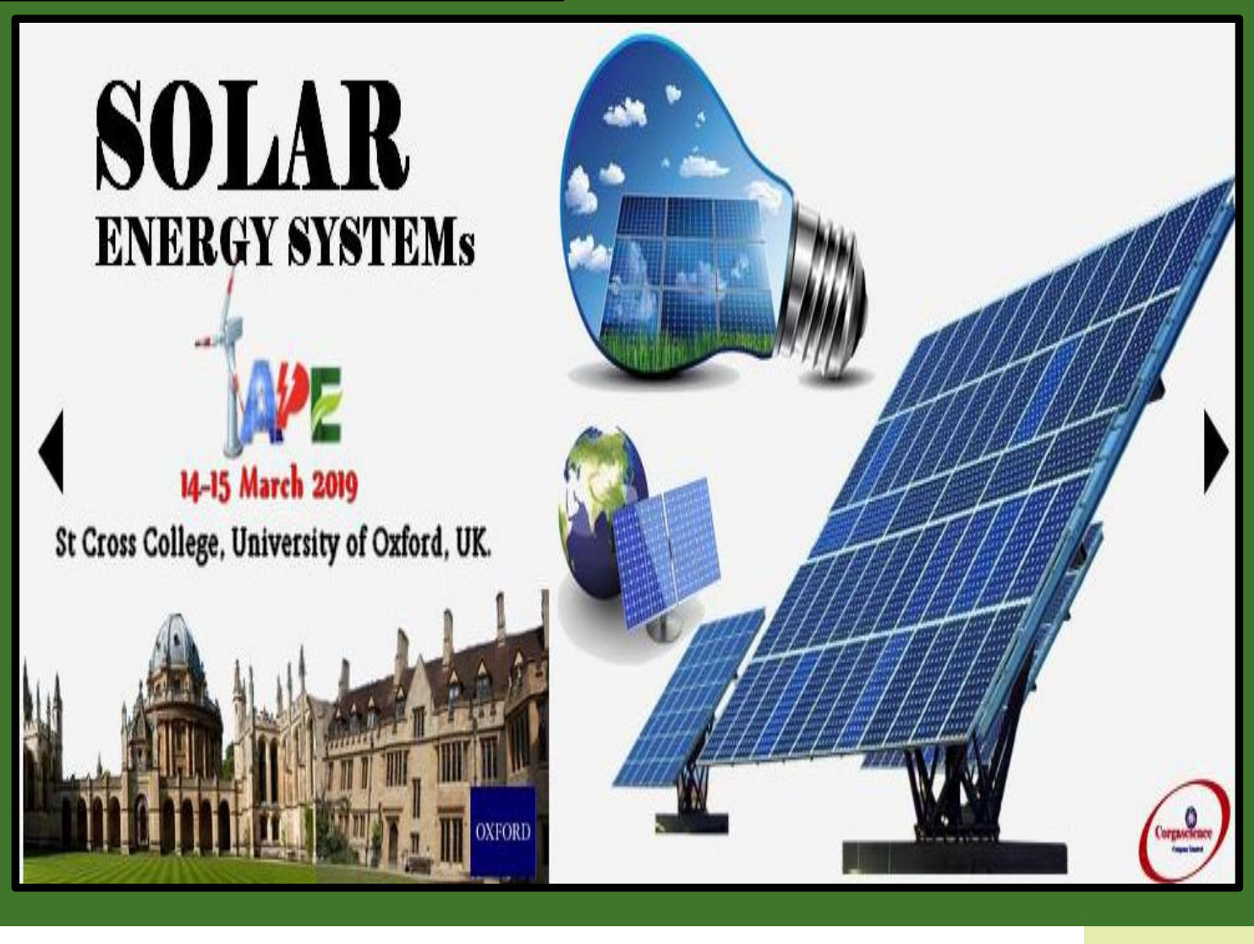

Miss Sireetorn Kuharat [1], Dr. O. Anwar Bég [1], Mr. Ali Kadir [1] and Dr. Meisam Babaie [2]*
[1]Aeronautical and Mechanical Engineering, University of Salford, Manchester, M54WT, UK
[3]Automotive & Autonomous Vehicle Technology (AAVT), University of Salford, Manchester, M54WT, UK.
*Poster Presenter

ABSTRACT

Nanofluids are currently being explored extensively in solar energy engineering to achieve improved performance in direct thermal absorber systems [1]. Nanofluids achieve significant enhancement in the heat transfer performance i.e. thermal efficiency. Motivated by these developments in nano-technology, in this poster we present recent simulations of steady-state nanofluid natural convection in a solar collector enclosure [2]. Two-dimensional, steady-state, incompressible laminar Newtonian viscous convection-radiative heat transfer in a rectangular solar collector enclosure geometry is modelled with **ANSYS FLUENT finite volume code (version 18.1)**. The enclosure has two adiabatic walls, one hot (solar receiving) and one colder wall. The Tiwari-Das volume fraction nanofluid model [3] is used and three different nanoparticles are studied (Copper (Cu), Silver (Ag) and Titanium Oxide (TiO_2)) and water base fluid. The solar radiative heat transfer is simulated in the ANSYS workbench, with the elegant P1 flux model and the Rosseland model. The influence of geometrical aspect ratio (AR) and solid volume fraction for nanofluids is also studied and a wider range is considered than in other studies. These constitute novel contributions in the area of solar nanofluid collectors since these aspects are considered collectively. Mesh-independence tests are conducted. Validation with published studies from the literature is included for the copper-water nanofluid case. The P1 model is shown to more accurately predict the actual influence of solar radiative flux on thermal fluid behaviour compared with Rosseland radiative model. With increasing Rayleigh number (natural convection i.e. buoyancy effect), significant modification in the thermal flow characteristics is induced with emergence of different vortex regions. With increasing aspect ratio (wider base relative to height of the solar collector geometry) there is a greater thermal convection pattern around the whole geometry, higher temperatures and the elimination of the cold upper zone associated with lower aspect ratio. Titanium Oxide nano-particles achieve higher temperatures and a greater local heat flux at the hot wall. Thermal performance can be optimized with careful selection of aspect ratio and nano-particles and this is very beneficial to solar collector designers. The modelling approach can be extended in future to consider fully three-dimensional simulations and unsteady effects.

MATHEMATICAL MODEL

Laminar, steady-state, incompressible flow is considered with forced convective heat transfer. The nanofluid is the absorber fluid and the Tiwari-Das nano-particle volume fraction model is deployed [3]**.** The fundamental equations take the following form:

D'Alembert mass conservation (2-D continuity):

$$\left[\frac{\partial u}{\partial x}+\frac{\partial v}{\partial y}\right]=0$$

x- and y- direction momentum conservation:

$$\left[u\frac{\partial u}{\partial x}+v\frac{\partial u}{\partial y}\right]=-\frac{1}{\rho}\frac{\partial p}{\partial x}+\ \nu\left[\frac{\partial^2 u}{\partial x^2}+\frac{\partial^2 u}{\partial y^2}\right]$$

$$\left[u\frac{\partial v}{\partial x}+v\frac{\partial v}{\partial y}\right]=-\frac{1}{\rho}\frac{\partial p}{\partial y}+\ \nu\left[\frac{\partial^2 v}{\partial x^2}+\frac{\partial^2 v}{\partial y^2}\right]-g[1-\beta(T-T)]$$

Energy conservation :

$$u\frac{\partial T}{\partial x}+v\frac{\partial T}{\partial y}=\alpha_m\left(\frac{\partial^2 T}{\partial x^2}+\frac{\partial^2 T}{\partial y^2}\right)+Q_{rad}$$

The ***Tiwari-Das model*** allows different concentrations (volume fractions) and types of metallic nano-particles to be studied. Nanofluid properties can be calculated from the following equations [3]**:**

$$\phi=\frac{v_{np}}{vf}\ ,\ \mu_{nf}=\frac{\mu f}{(1-\phi)^{2.5}}\ ,\ \rho_{nf}=(1-\phi)\rho f+\phi\rho s\ ,$$

$$C_{pnf}=\frac{(1-\phi)(\rho Cp)f+\phi(\rho Cp)}{\rho_{nf}},\ \frac{Knf}{kf}=\frac{ks+2kf-2\phi(kf-ks)}{ks+2kf-\phi(kf-ks)}$$

Here ϕ=volume fraction, V_{np}=nano particles volume and Vf =volume of fluid, μ_{nf}= dynamic viscosity of nanofluid (kg/m.s), μ_f= dynamic viscosity of base fluid, ρnf=nanofluid density, ρf=base fluid density, ρs =nanoparticle density, $Cpnf$=nanofluid specific heat, *knf* =nanofluid thermal conductivity, *kf* = fluid thermal conductivity and *ks* = nanoparticle thermal conductivity. The key local dimensionless parameters which may be computed in the post-processing in **ANSYS FLUENT** [4] are:

Rayleigh number: $Ra_x=\frac{g\beta}{V\alpha}(T_s-T_\infty)x^3$

Nusselt number: $Nu=\frac{hL}{k}=\frac{q''_{w\,CFD}(L)}{k(T_w-T_b)}$

Here *g* is gravity, β is coefficient of thermal expansion, α is thermal diffusivity, *x* is coordinate, *h* is convection coefficient, *L* is height of the enclosure, $q''_{w\,CFD}$ is numerical heat flux rate.

ANSYS FLUENT Boundary condition and radiation model

- Left wall: Constant temperature, T= 390 K
- Right wall: Constant temperature, T= 290 K.
- Top and Bottom walls: Adiabatic.

Radiative heat transfer is also incorporated using the ANSYS **P1 model** and **Rosseland** radiative models.

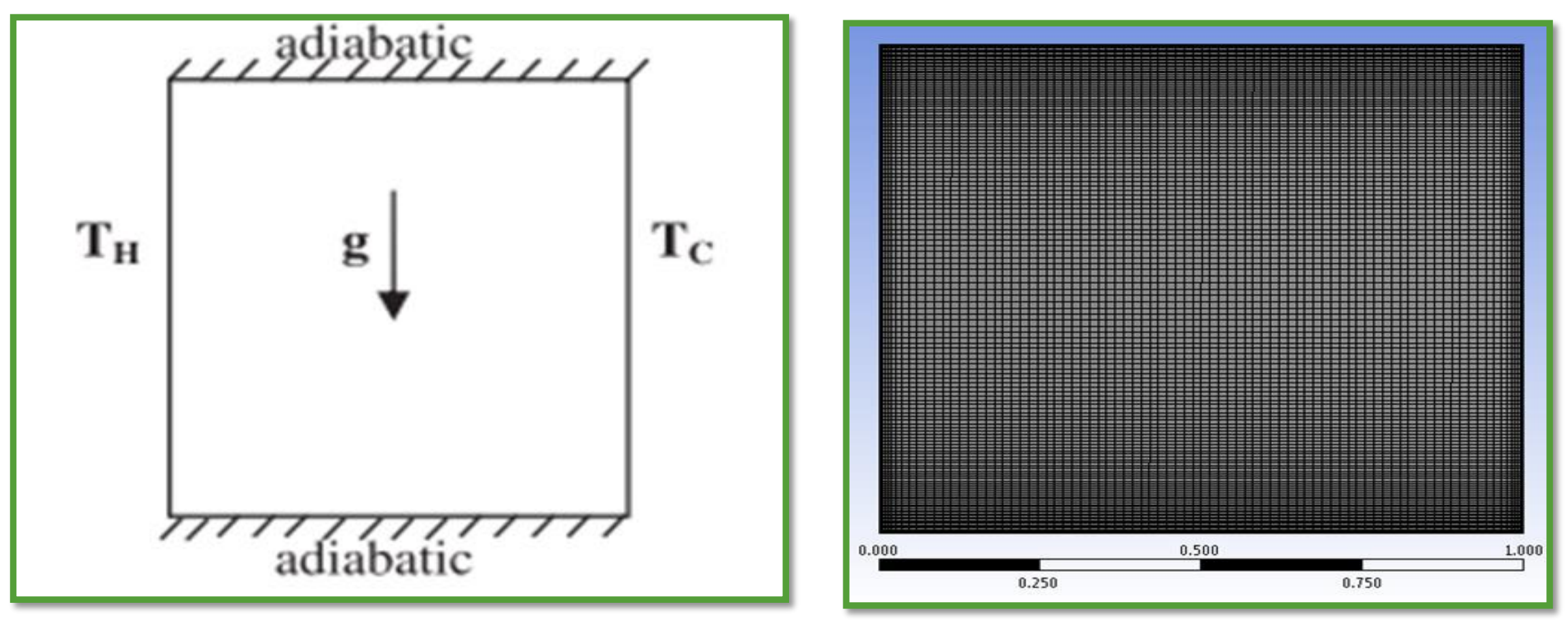

Fig 1, A-B: Enclosure geometry and CFD mesh

ANSYS FLUENT CFD METHOD

Simulations are executed in **ANSYS** software with the **SIMPLE** algorithm available with the pressure-based solver appropriate for incompressible flows). Quadrilaterals ("quad") elements have been used in the meshing process, (the square enclosure case is shown, AR = 1) in **Fig. 1.** Quad elements are commonly used in a simple geometry to reduce simulation times. **Fig. 2** illustrates the grid sensitivity analysis which shows that the simulations attain mesh-independent convergence with 10,000 elements.

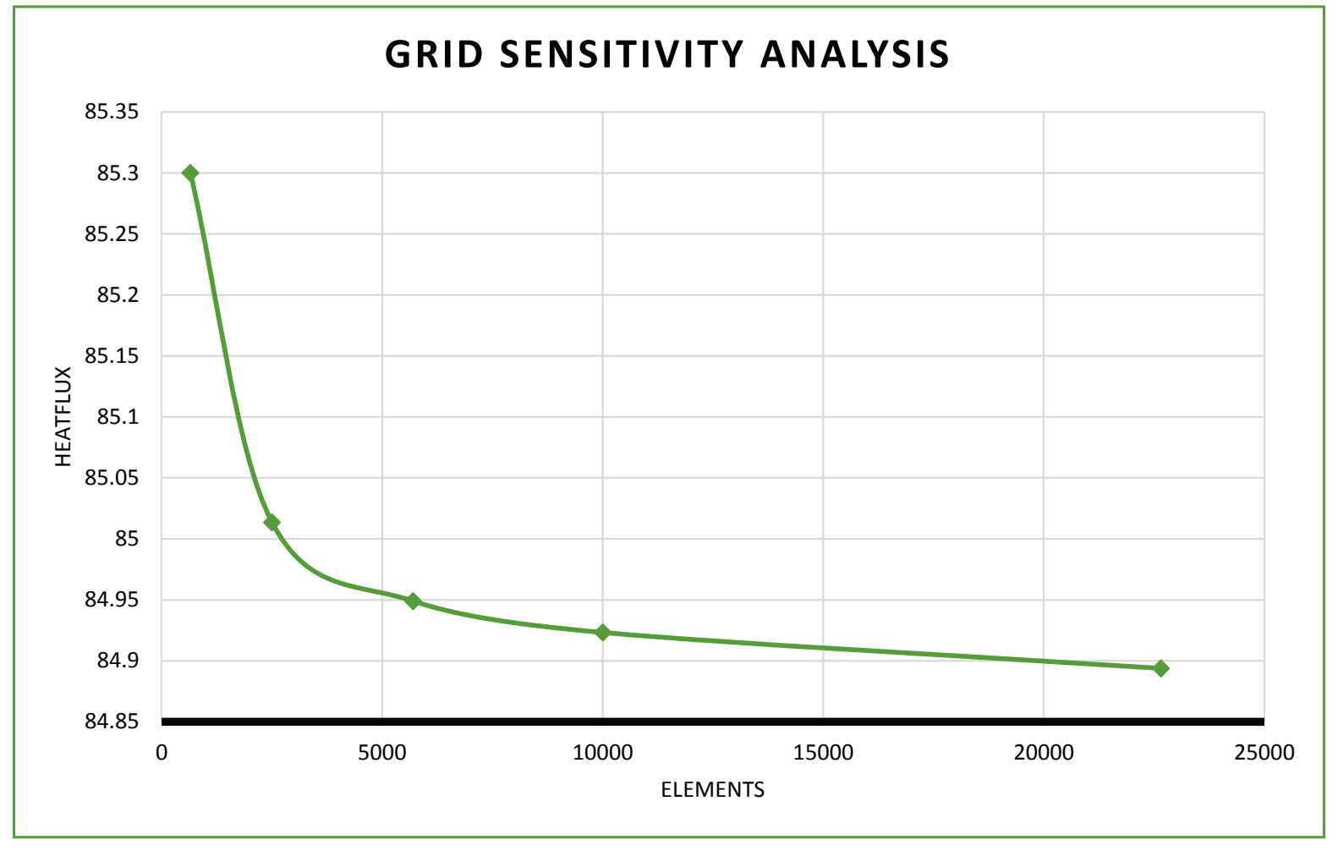

Fig. 2 Grid sensitivity analysis

VALIDATION

To validate the results obtained from the ANSYS Model for natural convection inside a 2-D enclosure filled with **copper-water nanofluid**, with a Rayleigh number of 10^3, a comparison is conducted with the earlier study of **Abu-Nada & Oztop** [5] for an aspect ratio of 1 (square enclosure) as shown in Fig. 3 A-B. The CFD simulation, using ANSYS FLUENT achieves close correlation with the results in [5] as testified to by the very close similarity in stream line and isotherm contour patterns. Other test cases were also conducted to further confirm confidence in the ANSYS FLUENT model. Once confidence was established in the simulations it is possible to progress with complexity in the geometry, buoyancy, nanofluid type and radiative effects.

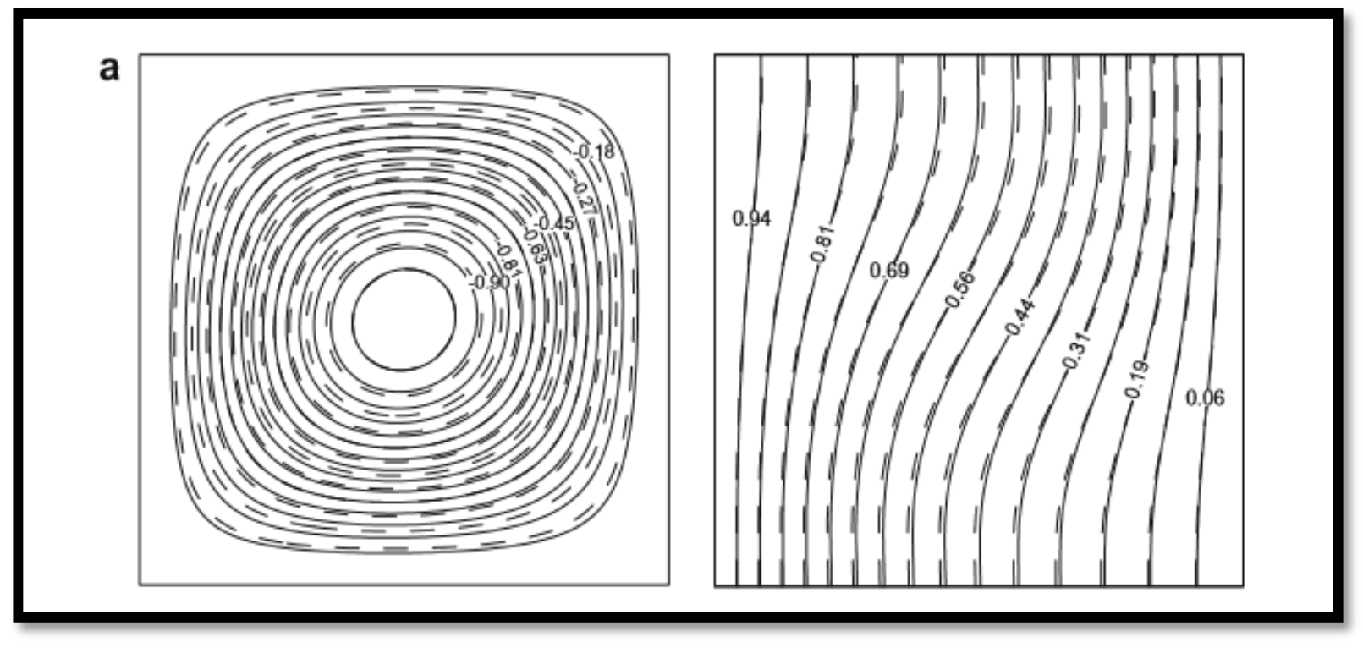

Fig 3 A finite volume results for Streamline and Isotherm plots for copper-water nanofluid, with a Rayleigh number of 10^3, volume fraction of 0.01 (Abu-Nada, E., & Oztop, H. 2009)

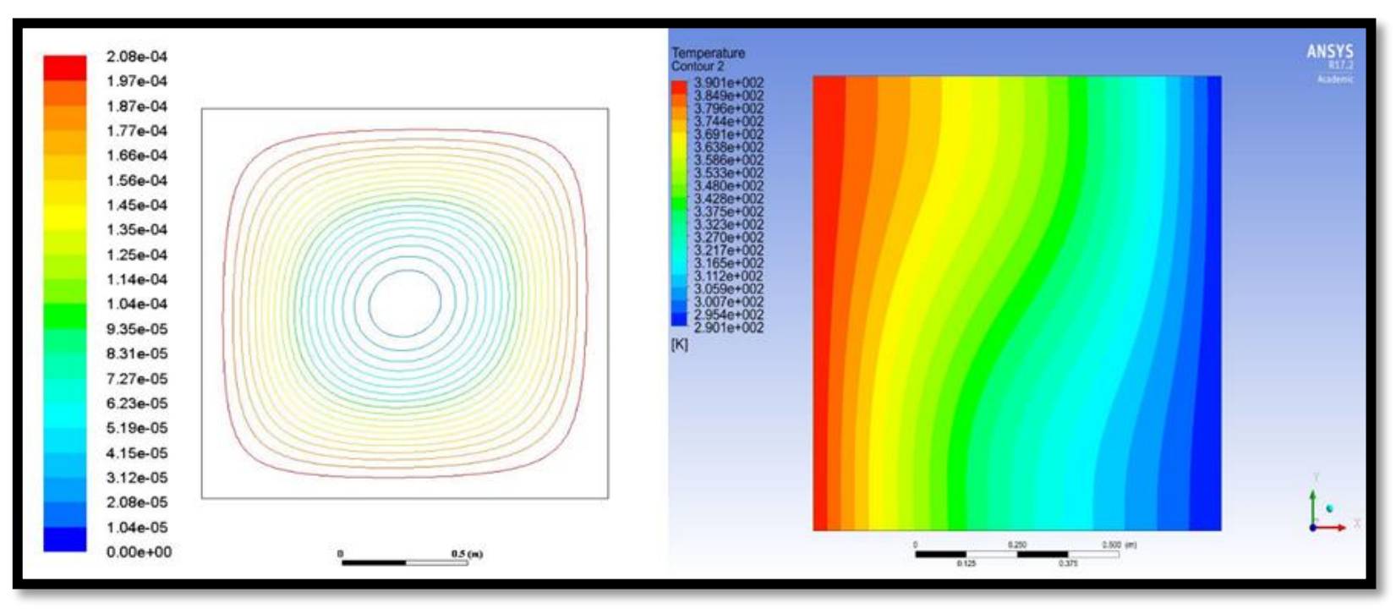

Fig 3 B ANSYS FLUENT Streamline and Isotherm plots for copper-water nanofluid, with a Rayleigh number of 10^3, volume fraction of 0.01

RESULTS

COMPARISON BETWEEN RADIATION FLUX MODELS

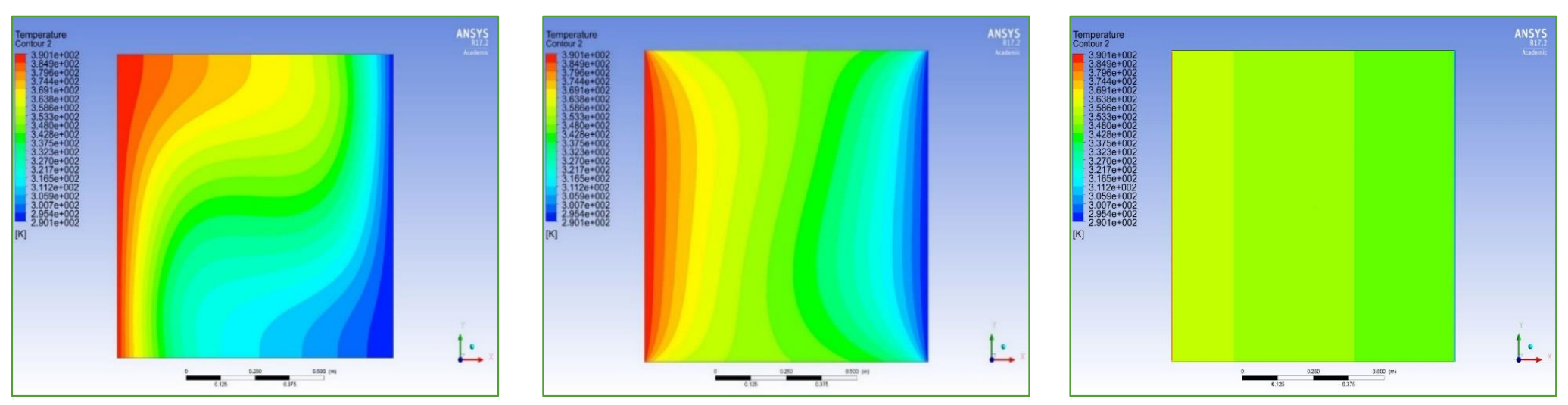

No radiation P1 radiation model Rosseland radiation model

Fig. 4 Temperature Contour of Silver-water (ϕ=0.04) at Ra=10^5

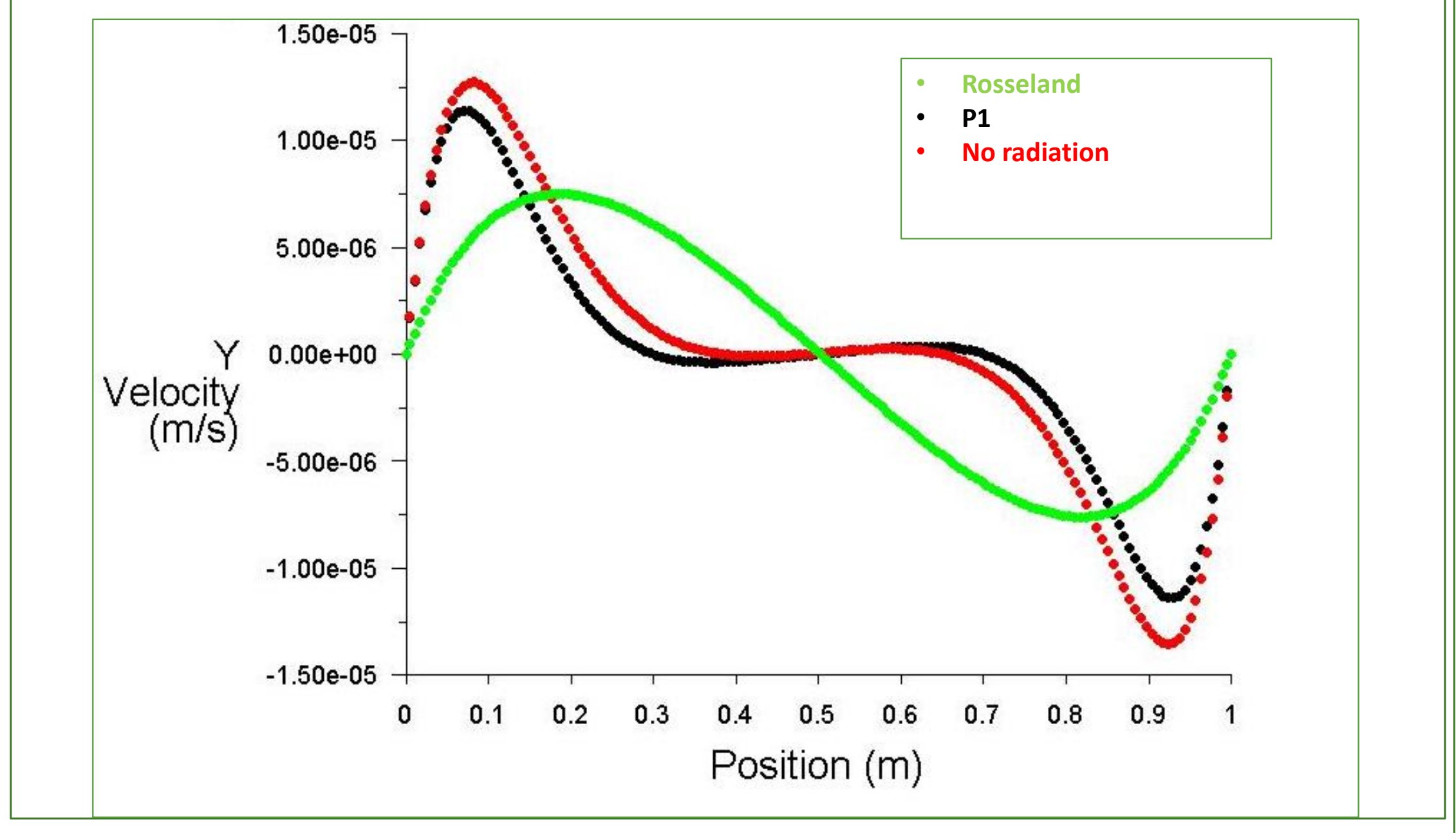

Fig. 5 Velocity distribution for Silver-water (ϕ=0.04) at Ra=10^5

COMPARISON OF HEAT TRANSFER RATES FOR DIFFERENT NANO-PARTICLES

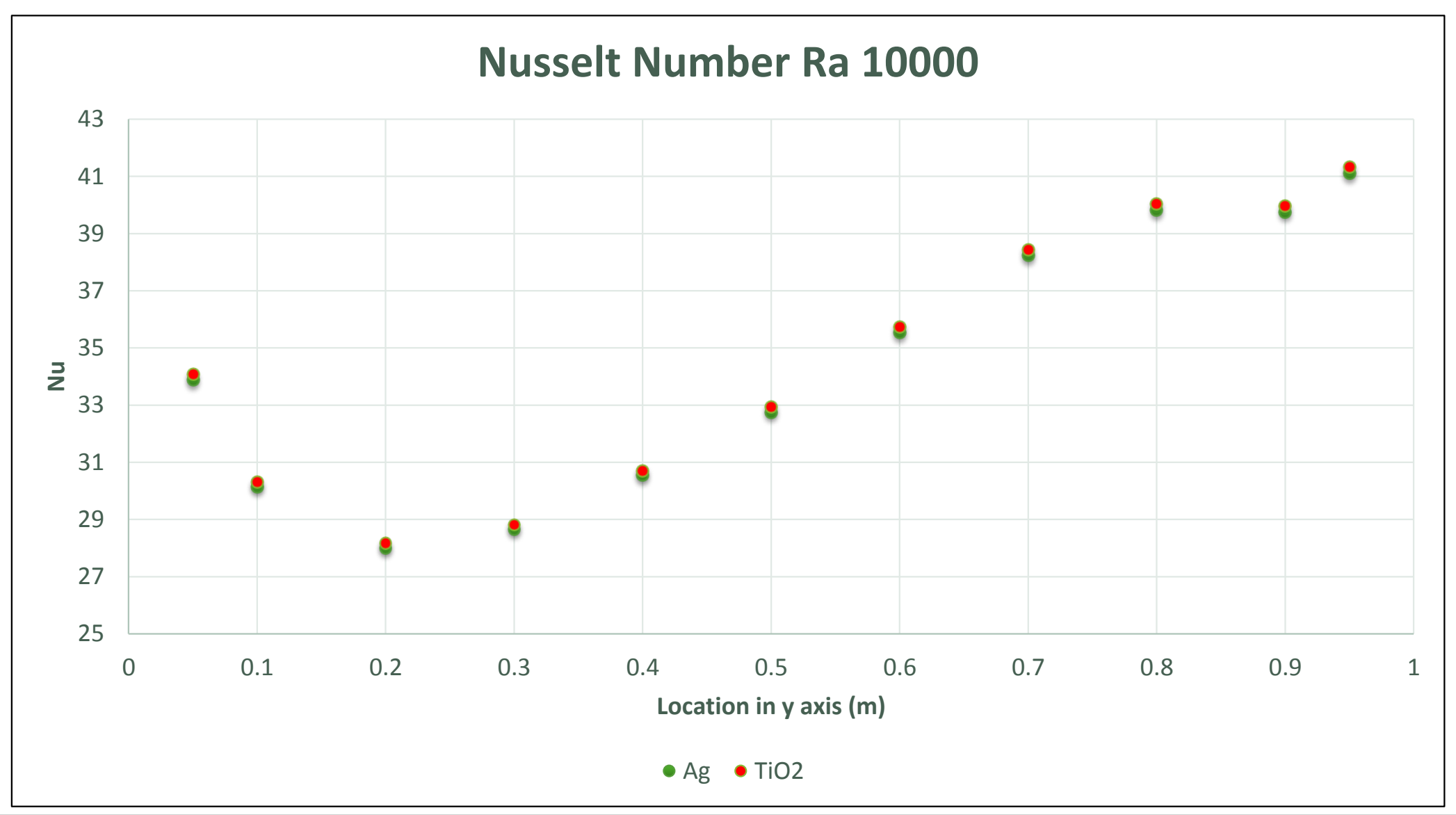

Fig. 6 Nusselt numbers for Titanium oxide-water and Silver-water (ϕ=0.04), Ra=10^4

COMPARISON OF ASPECT RATIO EFFECT FOR TITANIUM OXIDE-WATER

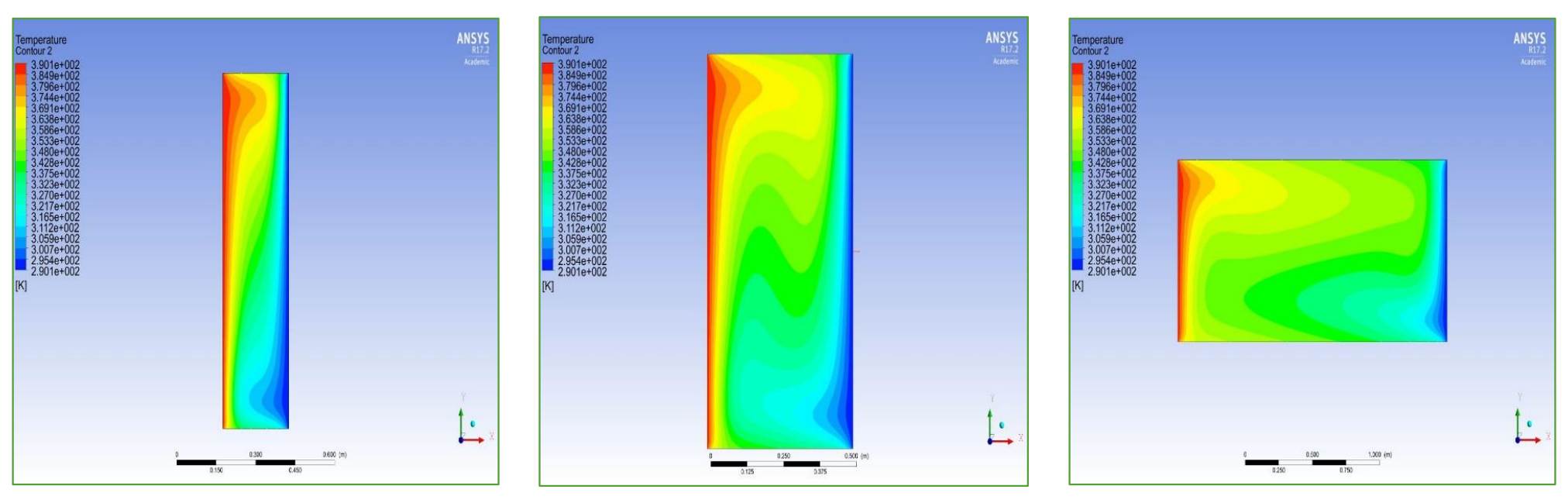

Aspect ratio of 4 Aspect ratio of 2 Aspect ratio of 0.5

Fig.7 Temperature Contours of Titanium oxide-water (ϕ=0.04) at Ra=10^5

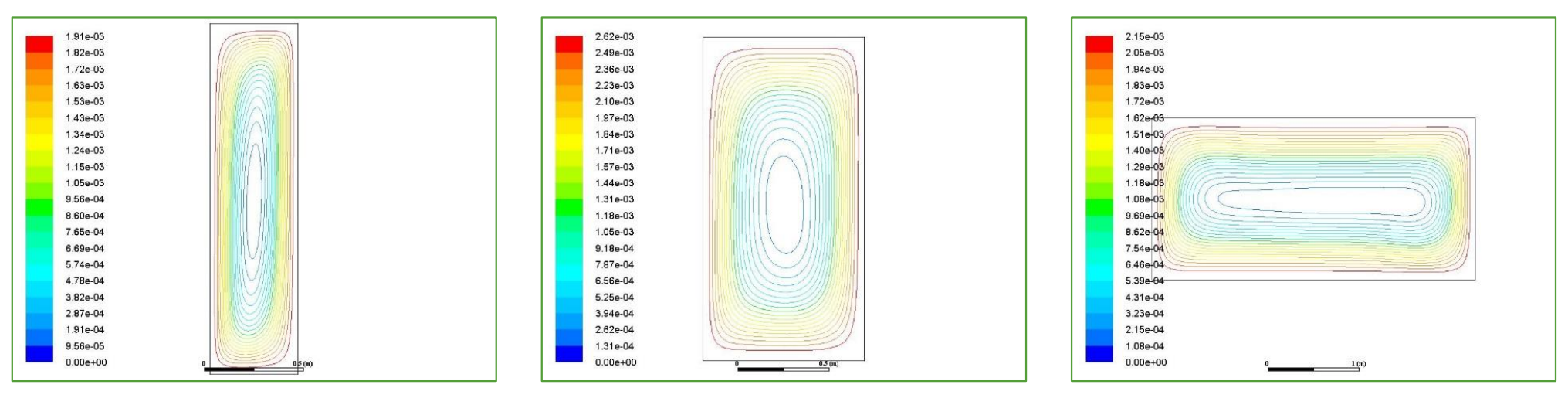

Aspect ratio of 4 Aspect ratio of 2 Aspect ratio of 0.5

Fig. 8 Streamlines of Titanium oxide-water (ϕ=0.04) at Ra=10^5

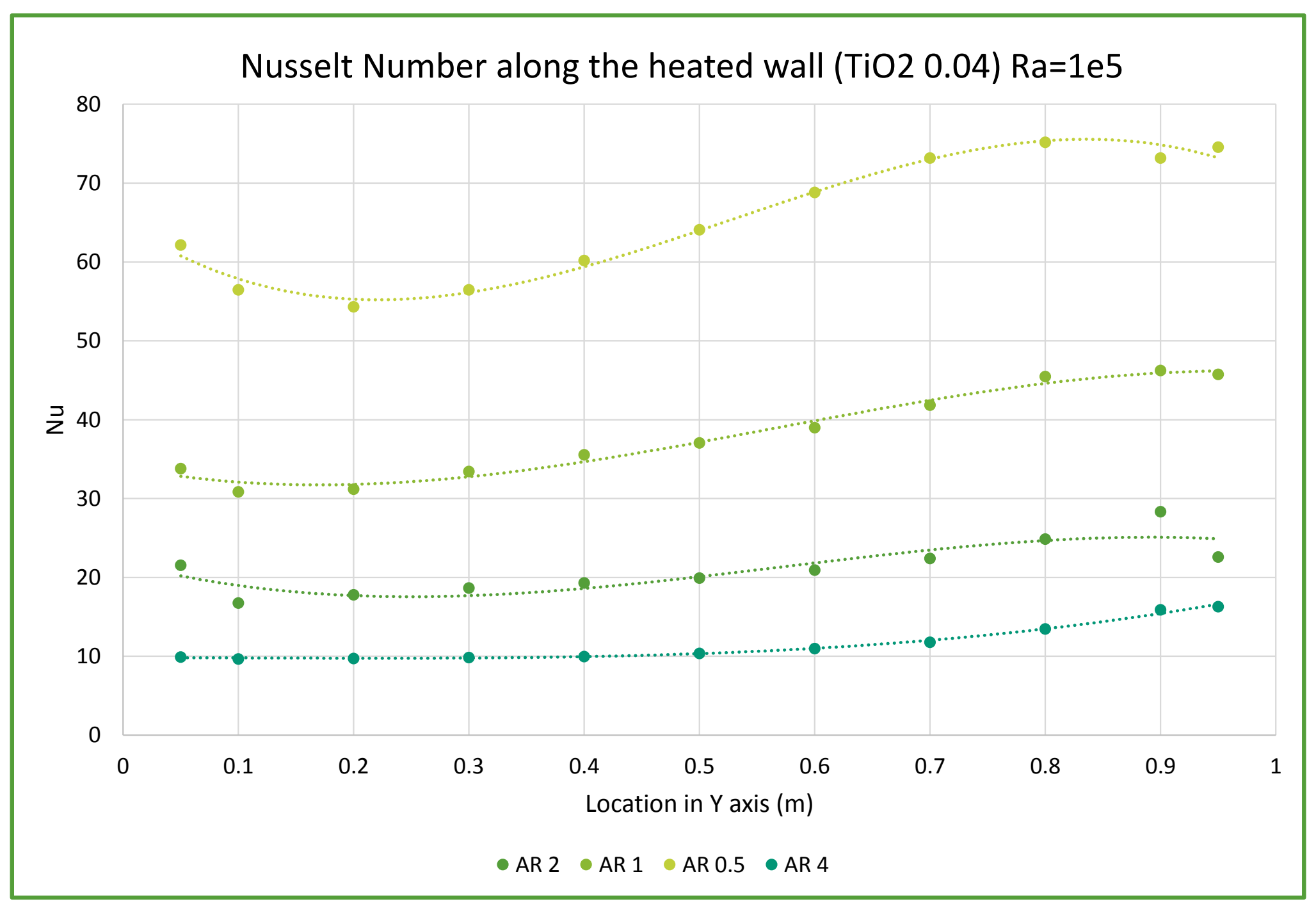

Fig. 9 Nusselt numbers for Titanium oxide-water (ϕ=0.04), Ra=10^4

CONCLUSIONS

- Results of selected simulations have been presented in **Figs. 3-9**.
- Simulations show that the Rosseland model predicts a temperature field (Figure 4) very different from that obtained without radiation. For the low optical thickness in this problem, the temperature field predicted by the Rosseland model is not physically realistic. The P-1 differential radiative model produces a more homogenous thermal effect adjacent to the hot wall and enables raditive flux to penetrate more evenly through the nanofluid enclosure, whereas the Rosseland model predicts a biased temperature enhancement only in the top left corner
- The P1 model yields the correct velocity profiles since the radiation source in the energy equation, which is proportional to the absorption coefficient, is small. The Rosseland model uses an effective conductivity to account for radiation, and yields the wrong temperature field, which in turn results in an erroneous velocity field.
- Deviations in the y-velocity profile are computed for the three cases of the Rosseland model, P1 model and no-radiation model. The P-1 velocity profiles accurately simulate the presence of a momentum boundary layer along the hot and cold walls. These concur with other studies in the literature [6].
- Higher Nusselt numbers (Fig. 6) are achieved for the Titanium Oxide water nanofluid compared with Silver water profiles are much closer to those obtained from nanofluid which is attributable to the higher thermal conductivity of the former.
- With decreasing aspect ratio (AR = ratio of height of enclosure to width of enclosure) there is significant expansion in the thermal dual zones at the upper and lower zones of the enclosure (Fig. 7). A more homogeneous temperature distribution is achieved at lower aspect ratio.
- At Rayleigh number, *Ra* = 10^5 the structure of streamlines suggest that the flow pattern is characterized by single cell circulation for all three aspect ratios considered (AR =4, AR = 2, AR = 0.5, Fig. 8). For *AR* = 0.5 the circulation is stronger than at the other aspect ratios. However at higher aspect ratio, the streamline distributions are more symmetrical than at the lowest AR value where dis-symmetry is observed and a skewness emerges in the circulation which is biased towards the left hot wall of the solar enclosure. Vortex structure is therefore clearly influenced by aspect ratio.
- Overall the isotherms are compressed towards the hot wall and the cold ceiling and most of the enclosure is occupied by warmer fluid at higher aspect ratios. Due to this effect, the single cell is expanded in both vertical and horizontal directions at higher aspect ratio with lesser distortion in the flow. This expansion results in boundary layer formation.
- Nusselt number at the left hot wall is maximized at low aspect ratio (AR =0.5) and minimized at high aspect ratio (AR =4) indicating that shorter and wider solar enclosures achieve significantly better heat transfer rates than taller and narrower enclosures.
- The present simulations provide a good benchmark for experimental studies and may also be generalized for other metallic nano-particles (gold, zinc etc) and extended to the unsteady case. These aspects are currently under consideration [7, 8].

Contact

Miss Sireetorn Kuharat MSc & Dr. O. Anwar Bég SMAIAA
Department of Aeronautical and Mechanical Engineering
University of Salford, Newton Building, The Crescent,
Manchester, M5 4WT, UK.
Email: S.Kuharat@edu.salford.ac.uk & O.A.Beg@salford.ac.uk

REFERENCES

1. O. Mahian *et al.,* A review of the applications of nanofluids in solar energy, ***Int. J. Heat Mass Transfer***, 57, 582-594 (2013).
2. **S. Kuharat**, An Investigation of Nanofluid Solar Collectors with Different Geometries using CFD Simulation, ***Year 1 PhD Interim Assessment Report, Aeronautical and Mechanical Engineering Department, University of Salford, Manchester, UK, November*** (2018).
3. R.K. Tiwari and M.K. Das, Heat transfer augmentation in a two-sided lid-driven differentially heated square cavity utilizing nanofluids. ***Int J Heat Mass Transfer***, 50, 2002–2018 (2007).
4. E. Abu-Nada and H.F. Oztop, Effects of inclination angle on natural convection in enclosures filled with Cu–water nanofluid, ***Int. J. Heat luid Flow***, 30 (4) 669-678 (2009).
5. Swanson Analysis Systems, ***ANSYS FLUENT Theory Manual, ver 18.1 Pennsylvania, USA*** (2018).
6. G. A. Sheikhzadeh and M. Nikfar, Aspect ratio effects of an adiabatic rectangular obstacle on natural convection and entropy generation of a nanofluid in an enclosure, ***J. Mechanical Science and Technology***, 27 (11) 3495-35 (2013) .
7. M. Notarianni et al., Plasmonic effect of gold nanoparticles in organic solar cells, ***Solar Energy***, 106, 23-37 (2014).
8. **S. Kuharat** and O. Anwar Bég, Simulation of aspect ratio effects on gold, titanium oxide, silver and zinc metallic-nano-particle water base solar collectors with CFD, ***Int. J. Energy Research*** (2018). ***In preparation.***